Fixed-vision based automated quality inspection and robotic nut sorting with Dobot Magician

Phisit Srinoi[1], Surasit Phokha[2], Viroch Sukontanakarn[1], Thewin Sakunbunyong[1], Wiriya Dangton[3]
[1]Field of Mechatronics Engineering, Faculty of Engineering, Rajamangala University of Technology Isan Khon Kaen Campus, Khon Kaen, Thailand
[2]Department of Mechanical and Mechatronics Engineering, Faculty of Engineering and Industrial Technology, Kalasin University, Kalasin, Thailland
[3]Field of Mechanical Engineering, Faculty of Engineering, Rajamangala University of Technology Isan, Khon Kaen, Thailand

Article Info

Article history:

Received Oct 19, 2025
Revised Jul 11, 2026
Accepted Jul 23, 2026

Keywords:

Classification accuracy
Dobot Magician
Image processing
Lighting effect
Machine vision
Nut sorting
OpenCV

ABSTRACT

This research presents a low-cost automated nut sorting system developed through laboratory testing to provide an affordable automation solution for small and medium enterprises (SMEs). The system integrates a fixed-vision camera with a Dobot Magician robotic arm, utilizing Python, OpenCV, and homography-based coordinate transformation for precise positioning. Performance was evaluated under three controlled lighting conditions with 25 samples each. Results indicate that lighting intensity significantly affects accuracy: low lighting (27.25 lux) yielded only 16% accuracy (mu=0.16, sigma approximately 0.3666), while high lighting (481.78 lux) suffered from overexposure and reflections. In contrast, optimal laboratory conditions (129.71 lux) achieved 100% classification accuracy (mu=1, sigma=0), demonstrating perfect consistency and stability. The study concludes that while the system offers a high-efficiency, budget-friendly alternative for SMEs, maintaining controlled, optimal illumination is critical for operational success. These findings provide a technical foundation for implementing cost-effective robotic sorting in real-world SME environments where high-cost sensor arrays are not feasible.

Corresponding Author:

Surasit Phokha
Department of Mechanical and Mechatronics Engineering
Faculty of Engineering and Industrial Technology, Kalasin University
62/1, Kasetsomboon Road, Muang District, Kalasin Province, 46000, Thailand
Email: surasit.ph@ksu.ac.th

1. INTRODUCTION

In modern manufacturing, ensuring the quality of mechanical components is paramount to maintaining product reliability and performance. As fundamental fasteners in various assemblies, nuts require stringent quality control measures to function effectively [1]–[3]. Traditional manual inspection methods, while historically standard, are increasingly viewed as time-consuming, prone to human error, and difficult to scale within high-throughput production environments. Consequently, there has been a significant shift toward automated systems that integrate machine vision and robotic technologies to enhance both the efficiency and accuracy of quality inspection and sorting processes [4]–[6].

Machine vision systems have become integral to quality control, utilizing advanced cameras and image processing algorithms to detect defects, measure dimensions, and verify component integrity. When integrated with robotics, these systems have revolutionized material handling; robotic arms equipped with vision capabilities can autonomously identify, pick, and place components with high precision [7]–[9].

Furthermore, the development of sorting robots demonstrates a remarkable versatility in handling diverse tasks. By leveraging image processing techniques to assess attributes such as color, shape, and texture, these systems can automate sorting, thereby reducing manual intervention and boosting overall throughput.

The Dobot Magician robotic arm has emerged as a versatile tool in both educational and industrial settings [10]. Its compact design and multi-functional capabilities make it ideal for tasks such as assembly and quality inspection. Integration with machine vision allows the Dobot Magician to perform complex tasks with high accuracy, ranging from academic demonstrations to industrial applications like sorting printed circuit boards (PCBs). Its adaptability and ease of programming make it an excellent platform for developing and testing scalable quality control solutions.

While existing literature demonstrates the feasibility of automated inspection, there remains a critical need for solutions that are both cost-effective and adaptable for small and medium enterprises (SMEs) [11]. In the era of Industry 4.0, SMEs often face barriers to adopting advanced technologies due to high investment costs and limited operational space. This research addresses this gap by presenting an automated quality inspection and robotic nut sorting system using fixed-vision and the Dobot Magician. A key technical distinction of this work is the implementation of a fixed-mount (stationary) camera system, which overcomes the limitations of 'eye-in-hand' configurations found in many previous studies. Unlike eye-in-hand systems—where the robot must stop to capture stable images—the fixed-vision approach enables real-time image processing while the robot remains in motion. This approach significantly reduces cycle times, simplifies coordinate transformation (calibration), and provides a stable environment for detecting surface defects and dimensional accuracy using Python and OpenCV [12]. By leveraging open-source software and accessible hardware, this system provides a scalable model for automated quality control in nut manufacturing.

The primary objectives of this research are to develop an image processing-based framework capable of precisely distinguishing between high-quality and defective nuts, and to implement a robust fixed-vision coordination system for the Dobot Magician to execute autonomous pick-and-place tasks based on real-time visual data. Furthermore, the study aims to enhance the competitive edge of SMEs by reducing labor dependency and increasing production throughput, while concurrently evaluating the system's performance in terms of classification accuracy and processing speed under varying operational conditions [13].

As illustrated in the comparison Table 1, while traditional image processing and deep learning offer high accuracy, they often come with high costs or complex configurations that are not suitable for SMEs. Furthermore, many existing integrated robotic sorting systems rely on 'Fixed Vision' configurations, which suffer from increased cycle times. In contrast, the proposed system leverages the affordability of the Dobot Magician combined with a fixed-vision approach [14]–[16]. This integration fills the gap by providing a cost-effective, high-speed solution that maintains stability and precision, making it an ideal model for small-scale industrial application.

Table 1. Comparison of related works in automated inspection and sorting

Research focus	Methodologies/techniques	Key findings/strengths	Limitations/research gap
Traditional image processing [12], [17]	Edge detection, hough transform, and morphological operations	Effective for basic dimensional measurement and geometrical features.	Vulnerable to lighting changes; less effective for complex defects.
Advanced pattern recognition [18], [19]	Feature extraction, template matching, and pattern recognition	High consistency in detecting minor surface defects on metallic parts.	Requires high computational power; often difficult for SMEs to implement.
Deep learning (AI) [18], [20]	Convolutional neural networks (CNNs)	Superior accuracy in classifying defective vs. non-defective components.	High cost of data labeling and hardware requirements; complex setup.
Integrated robotic sorting [14], [21]	Vision-guided pick-and-place, conveyor belt integration	Significantly reduces processing time and increases throughput.	Most studies use expensive industrial robots or "Eye-in-Hand" systems.
Educational and desktop robotics [10], [22]	Dobot Magician, OpenCV, Python, and Block-based coding	High affordability, versatile, and user-friendly for research/training.	Primarily used in education; needs more validation for industrial SME tasks.
Proposed system (our work)	Fixed-Vision+Dobot Magician+Python/OpenCV	Low-cost, real-time processing (no motion delay), and scalable for SMEs.	Focuses specifically on fixed-mount stability for high-speed nut sorting.

Image processing and machine vision have become indispensable tools in industrial quality inspection, providing a level of accuracy and consistency that manual inspection cannot sustain. Previous research has shown that techniques ranging from traditional edge detection to advanced deep learning models are effective in identifying defects and measuring dimensional accuracy in mechanical parts. Furthermore, the integration of these vision systems with robotic manipulators has proven to be a successful strategy for autonomous sorting and material handling. However, a significant gap remains in the availability of systems that are both high-performing and accessible to SMEs. Many existing industrial solutions utilize 'Fixed Vision' configurations that increase cycle times or rely on expensive, high-end robotics [23]. The Dobot Magician, as highlighted in recent studies, offers a versatile and cost-effective platform that bridges the gap between educational research and practical application. By synthesizing these findings, this research adopts a fixed-vision approach to overcome the efficiency limitations of mobile-camera systems. Leveraging the stability of stationary image processing combined with the precision of the Dobot Magician, the proposed system aims to provide a scalable, real-time, and low-cost solution for nut sorting [24]. These theoretical foundations and technological precedents set the stage for the system design and experimental methodology detailed in the following chapter.

2. MATHEMATIC EQUATIONS RELATED TO THE RESEARCH

In the context of robotic pick-and-place systems, lighting is the most critical environmental factor affecting the reliability of computer vision. Here is an explanation of its impact and the mathematical foundations involved.

2.1.1. Camera-to-robot coordinate transformation

To enable precise robotic pick-and-place operations, the system employs a homography matrix H to map 2D pixel coordinates (x, y) into real-world robot coordinates (X_r, Y_r), as expressed in (1) [25]:

$$\begin{bmatrix} X_r \\ Y_r \\ 1 \end{bmatrix} = H \begin{bmatrix} x \\ y \\ 1 \end{bmatrix}, (X_r, Y_r) = \left(\frac{h_{11}x + h_{12}y + h_{13}}{h_{31}x + h_{32}y + h_{33}}, \frac{h_{21}x + h_{22}y + h_{23}}{h_{31}x + h_{32}y + h_{33}} \right) \tag{1}$$

where (x, y) are the pixel coordinates in the camera frame, (X_r, Y_r) are the corresponding robot workspace coordinates, and h_{ij} are the elements of the homography matrix H obtained through prior calibration. This transformation ensures sub-millimeter alignment between the visual coordinate frame and the robot workspace.

2.1.2. Environmental impact of lighting on image analysis

Lighting directly dictates the quality of the "input data" (the image) that your algorithms must process. Poor lighting conditions lead to several technical failures:

- Signal-to-noise ratio (SNR): in low-light conditions, the camera sensor increases its "gain," which introduces digital noise. This noise creates graininess that can be misinterpreted as edges or textures, leading to unstable coordinate data.
- Specular reflection (Glint): when working with metallic or glossy workpieces, direct lighting causes "hotspots." These bright spots saturate pixels (making them pure white), which destroys the geometric information of the object's surface and shifts the calculated centroid (center point).
- Shadow interference: harsh, directional lighting creates shadows that the software may perceive as part of the object's geometry. This results in a "bounding box" that is larger than the actual part, causing the robot gripper to collide or miss.
- Chromatic shift: if the ambient light color temperature changes (e.g., sunlight vs. factory light emitting diode (LED)), the hue, saturation, and value (HSV) values of the workpiece will drift. This makes color-based sorting algorithms fail if they rely on static thresholds.

2.1.3. Mathematical equations involved

To bridge the gap between a 2D image and a 3D robot movement, several equations are sensitive to lighting:

a. Image segmentation (thresholding)

The process of separating the workpiece from the background depends on the intensity function $f(x, y)$. If lighting is inconsistent, a fixed threshold T fails as shown in (2):

$$g(x, y) = \begin{Bmatrix} 1 & if\ f(x, y) > T \\ 0 & if\ f(x, y) \leq T \end{Bmatrix} \tag{2}$$

In dynamic lighting, engineers often use adaptive thresholding, where T is calculated locally for every pixel based on its neighbors, helping to compensate for uneven illumination.

b. Centroid calculation (moments)

To send a coordinate to the robot, we must find the center of the detected object using Image Moments (M_{ij}) as shown in (3) [26]:

$$M_{ij} = \sum_x \sum_y x^i y^i I(x,y) \quad (3)$$

The pixel coordinates $(\bar{x}, \bar{y})$ of the center as shown in (4):

$$\bar{x} = \frac{M_{10}}{M_{00}}, \qquad \bar{y} = \frac{M_{01}}{M_{00}} \quad (4)$$

If shadows or reflections change the intensity $I(x,y)$ of even a few pixels, the calculated $(\bar{x}, \bar{y})$ shifts. Even a 2-pixel error in a high-mounted camera can translate to several millimeters of error in the robot's physical workspace.

c. The pinhole camera model (coordinate projection)

The transformation from image pixels (u, v) to real-world coordinates (X_w, Y_w, Z_w) is defined by the camera matrix as shown in (5) [27]:

$$s = \begin{bmatrix} u \\ v \\ 1 \end{bmatrix} = K[(R|t)] \begin{bmatrix} X_w \\ Y_w \\ Z_w \\ 1 \end{bmatrix} \quad (5)$$

where K contains intrinsic parameters (focal length, optical center). If lighting causes vignetting (darkening at the corners) or affects the clarity of calibration patterns (like checkerboards), the matrix parameters will be inaccurate, leading to systematic "offset" errors in the robot's reach.

3. MATERIAL AND METHOD

This section presents the materials and method used to develop the automated nut inspection and robotic sorting system. It integrates computer vision, calibration techniques, and robotic manipulation to achieve accurate real-time classification and handling.

3.1. System operation description

The proposed automated nut inspection and robotic sorting system integrates computer vision, geometric calibration, and robotic manipulation to enable accurate nut classification and handling in real-time. The system architecture is implemented in Python using the OpenCV, NumPy, and PyDobot libraries [28], in conjunction with serial communication to control peripheral hardware such as the Dobot Magician robotic arm and an Arduino-based pneumatic actuator [22]. Figure 1 illustrates the proposed system, which integrates a computer vision pipeline with robotic automation to achieve high-precision industrial nut sorting [18]. The process begins with system initialization and ROI configuration, followed by a 30-ms high-speed loop that captures frames and performs HSV color transformation [17]. A decision logic module then filters identified objects based on size and predefined metric references to ensure sorting accuracy. Once a target is confirmed, a homography transformation converts image pixels into real-world coordinates for the robotic manipulator. The system executes a sequence of hardware actions, including stopping the conveyor belt and triggering the Dobot arm via serial communication. Finally, all operations are visualized through a PyQt5 graphical user interface (GUI), while performance data and robot trajectories are logged for real-time monitoring and analysis [29].

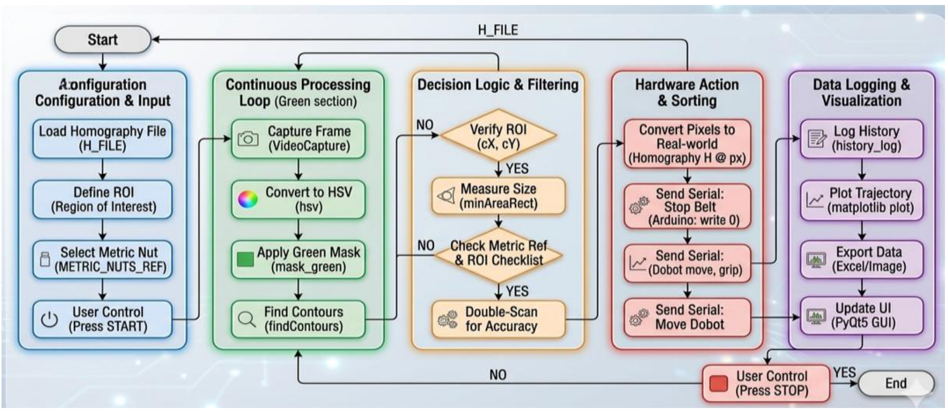

Figure 1. System architecture of an automated vision-based nut sorting robot

The experimental setup includes a PC running Python and OpenCV to control a Dobot Magician robotic arm with a gripper, a high-resolution camera for image capture, and calibration tools for pixel-to-robot mapping. Figure 2 illustrates the system configuration, where a conveyor belt driven by a 24 V DC motor via an Arduino and relay module carries nuts for inspection. The system classifies nuts into target (e.g., M10) and non-target types, sorting them into separate boxes, with solid lines indicating power connections and dashed lines indicating data communication [19]. The Dobot Magician is a versatile desktop robotic arm equipped with stepper motors, designed to perform tasks such as pick-and-place operations.

The schematic diagram of the system, shown in Figure 3 consists of a PC running Python and OpenCV that communicates with a Dobot Magician robot equipped with a gripper and an HD digital camera. The PC processes image data to identify the target object (Nut M6) on the conveyor belt. The Dobot Magician then picks up the detected nut and places it into Box 1 (Target). An Arduino Uno controls the conveyor belt's 24 V DC motor via a relay module, all powered by an electric supply, while Box 2 serves as the non-target container.

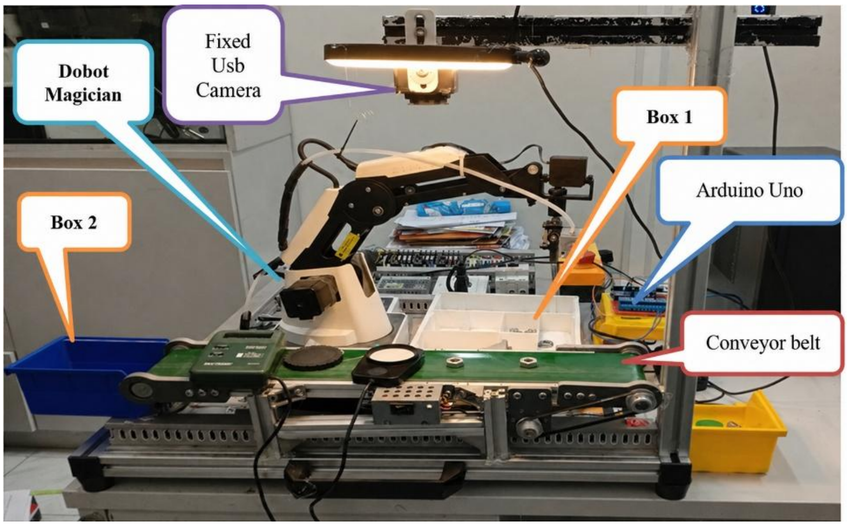

Figure 2. Hardware setup of the automated nut sorting system

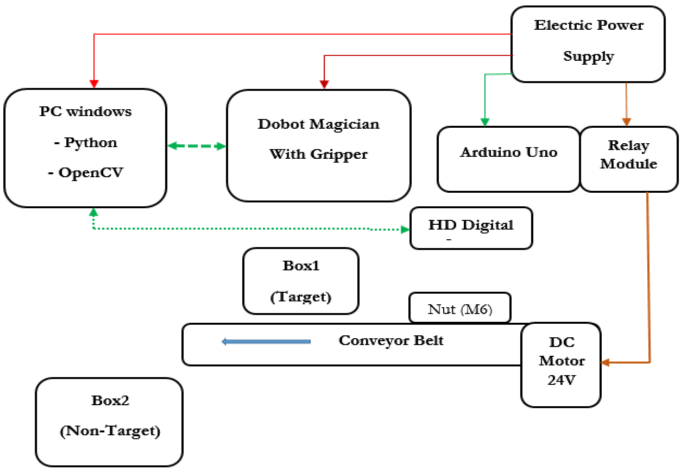

Figure 3. Schematic diagram of the automated nut sorting system

The independent variables in the experiment include nut type (standard and defective), lighting condition (bright, dim, and mixed), and nut orientation on the table. The dependent variables comprise the detection accuracy of the vision system—measured as the percentage of correctly classified nuts—the sorting success rate, defined as the percentage of nuts correctly picked and placed by the Dobot Magician, and the average cycle time per nut in seconds. Figure 4 shows the drawing and dimensions of the nut.

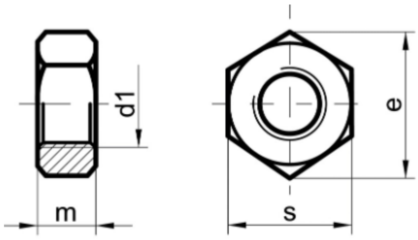

Figure 4. Dimensional of a hex nut

Table 2 presents the standard dimensions of hexagonal nuts ranging from M6 to M12 according to ISO 4032 (Hexagon nuts, style 1–Product grades A and B), including thread diameter, pitch, across flats, and nut height.

Table 2. Standard dimensions of hex nuts (M6–M12) according to ISO 4032: Hexagon nuts, style 1

Nut size	Thread dia.,d_1 (mm)	Pitch (mm)	Across flat, s (mm)	Nut height, m (mm)
M6	6.0	1.0	10.0	5.0
M8	8.0	1.25	13.0	6.5
M10	10.0	1.50	17.0	8.0
M12	12.0	1.75	19.0	9.8

3.2. Preparation of the experimental environment

In this experiment, we divided the lighting conditions into three levels to study the effects of illumination on the robot's object picking performance [30]. Figure 5 illustrates the preparation of the experimental environment with varying illuminance levels for comparison, where Figure 5(a) shows the setup under low light conditions (2.5 fc=27.25 lux) to simulate dim lighting, Figure 5(b) presents the setup under the target light conditions (129.71 lux) representing typical indoor illumination, and Figure 5(c) depicts the setup under high light conditions (481.78 lux) to evaluate performance under bright lighting. A program was used to inspect workpieces (hexagonal nuts) based on their size; objects that are not nuts are not initially detected, as shown in Figure 6.

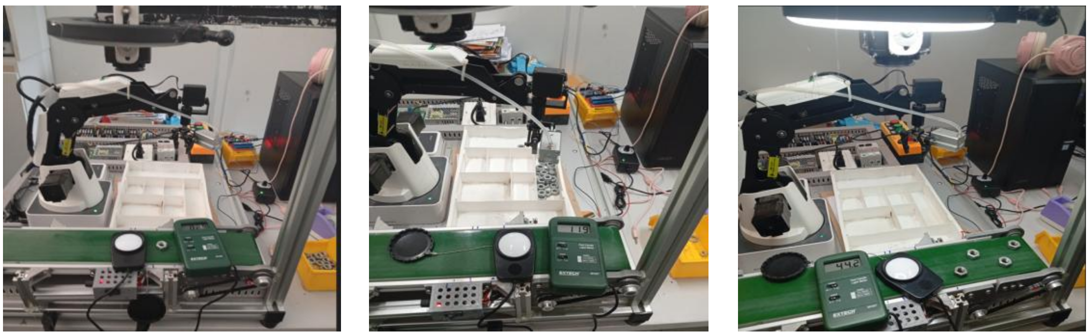

(a) (b) (c)

Figure 5. Experimental setup under different lighting conditions; (a) low light (2.5 fc=27.25 lux), (b) target light (129.71 lux), and (c) high light (481.78 lux)

3.3. Eye-to-hand camera calibration

This section describes the eye-to-hand calibration process using a stationary overhead camera and the Dobot Magician [20], [21], [31]. The procedure is illustrated in Figure 7. Figure 7(a) shows the experimental workspace, which consists of a Dobot Magician positioned at a conveyor belt with a camera mounted on an overhead frame to provide a fixed top-down view. In Figure 7(b), ground-truth data is gathered by manually guiding the robot's end-effector to specific targets on the belt, establishing the physical relationship between the robot's coordinates and the camera's visual field. Figure 7(c) displays a custom Python-based GUI, "Dobot 6-Point Calibration Control," which maps image coordinates (u, v) to robot coordinates (x, y, z). These point pairs are used to compute the homography matrix, enabling the system to translate visual detection into precise robotic movement.

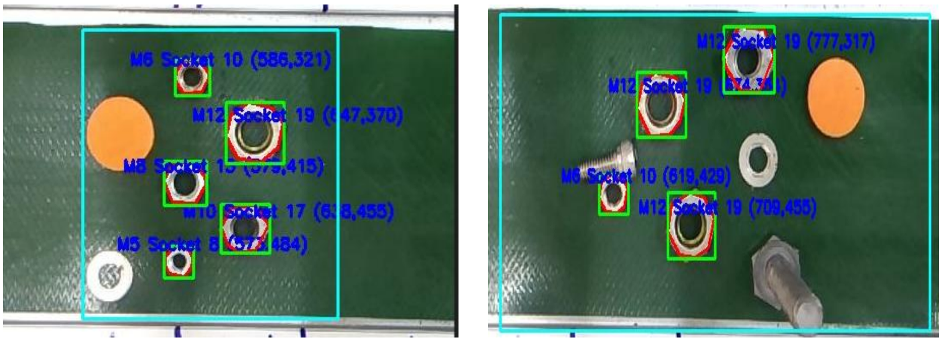

Figure 6. The detection of nuts and non-nut objects using the designed program

(a) (b) (c)

Figure 7. Eye-to-hand calibration process; (a) experiment setup, (b) manual data collection, and (c) 6-point coordinate mapping

4. RESULTS AND DISCUSSION

The results from the experiment on picking and sorting screws, achieved through the collaboration between computer vision and the Dobot Magician—a small-sized robot used for basic demonstration purposes—can be presented in three ways according to the light intensity, which affects the camera's detection. The camera, fixed in position, sends the coordinates to the robot as follows:

4.1. Experiment at low lighting effect

This experiment evaluates the robustness and reliability of the object detection and sorting system under sub-optimal lighting conditions. As environmental illumination significantly impacts image preprocessing and contour detection, the system was tested in a low-light environment (e.g., <100 lux) to determine the error rate in coordinate mapping. Table 3 records the performance of a robotic pick-and-place system under dim lighting (27.25 lux). It includes data on the size of the objects, camera and robot coordinates, pick errors, drop targets, and cycle times.

a. Data summary by workpiece size

Based on the 25 bolt-picking trials, the analysis demonstrates the system's robustness against potential misidentification caused by low lighting conditions. When categorizing the data by workpiece size, clear clustering in coordinates and cycle times is highly evident:

- Total samples: 25 units
- Target bolt size: M10
- Successful M10 identifications: 4
- Misidentified as other sizes (M12, M16): 21
- Error rate: 84%

Due to insufficient ambient lighting, the vision system experienced significant difficulty in distinguishing the target M10 bolts from other sizes. Out of a total of 25 bolts processed, the robot correctly identified the M10 size only 4 times, resulting in a misidentification of 21 units as either M12 or M16. This represents a substantial classification error of 84%, as the system incorrectly read the bolt dimensions under poor contrast. Statistically, the standard deviation (SD) of the classification error for selecting the wrong bolt size is calculated at approximately 0.37 (based on a binary success/fail distribution). The low light levels likely blurred the edge detection of the threads, leading the robot to default to the larger M12 profile in 20 instances and M16 in one instance. Consequently, the accuracy fell far below the required threshold for the M10 production line. To resolve this, the illumination must be increased to reduce the optical noise and lower the error variance. In this context, if we treat a correct pick (M10) as 1 and a wrong pick as 0:

- Mean (μ): 4/25=0.16
- Variance (σ^2): P(1-P)=0.16×0.84=0.1344
- SD (σ): $\sqrt{0.13440} \approx 0.3666$

Table 3. Record data from experiment (low lighting: 27.25 lux)

Size	Cam_X	Cam_Y	Robot Actual_X	Robot Actual_Y	Pick error	Target Drop_X	Target Drop_Y	Cycle_Time (s)
M12	155.91	-154.33	155.91	-154.33	0	168.13	155	12.58
M12	155.21	-165.27	155.21	-165.27	0	168.13	155	12.88
M12	154.53	-158.72	154.53	-158.72	0	168.13	155	12.58
M12	159.04	-162.64	159.04	-162.64	0	168.13	155	12.58
M12	155.73	-144.14	155.73	-144.14	0	168.13	155	12.59
M10	157.96	-168.54	157.96	-168.54	0	200	50	11.68
M12	151.6	-142.87	151.6	-142.87	0	168.13	155	12.59
M12	161.67	-174.4	161.67	-174.4	0	168.13	155	12.89
M10	151.7	-131.13	151.7	-131.13	0	200	50	11.37
M10	160.93	-179.06	160.93	-179.06	0	200	50	11.68
M12	157.01	-154.35	157.01	-154.35	0	168.13	155	12.58
M12	154.16	-162.54	154.16	-162.54	0	168.13	155	12.89
M12	151.95	-141.72	151.95	-141.72	0	168.13	155	12.59
M10	161.33	-175.44	161.33	-175.44	0.0001	200	50	11.68
M12	152.35	-146.91	152.35	-146.91	0	168.13	155	12.59
M12	161.3	-172.3	161.3	-172.3	0	168.13	155	12.88
M12	151.41	-138.8	151.41	-138.8	0	168.13	155	12.58
M12	159.59	-177.49	159.59	-177.49	0	168.13	155	12.87
M12	155.11	-140.66	155.11	-140.66	0	168.13	155	12.58
M12	157.42	-168.53	157.42	-168.53	0	168.13	155	12.88
M12	154.64	-159.28	154.64	-159.28	0	168.13	155	12.59
M12	153.29	-142.92	153.29	-142.92	0	168.13	155	12.59
M12	158.1	-166.4	158.1	-166.4	0	168.13	155	12.89
M16	152.3	-140.57	152.3	-140.57	0	150	70	11.98
M12	154.32	-174.82	154.32	-174.82	0	168.13	155	12.88

b. Trends analysis:
- Coordinate calibration and accuracy validation: the most prominent trend is that the camera-detected coordinates (Cam_X, Cam_Y) and the actual robot coordinates (Robot Actual_X, Robot Actual_Y) are nearly identical. This results in a Pick Error of zero or near-zero, proving that the Homography Matrix Calibration between the computer vision system and the robotic arm achieved exceptional accuracy, effectively eliminating spatial transformation errors.
- Cycle time trends:

i) The M10 group achieved the shortest average cycle time (~11.60 seconds).
ii) The M12 group required the longest average cycle time (~12.70 seconds).
iii) Observation: the variance in cycle time is not directly dictated by the physical size of the workpiece. Instead, it correlates with the travel distance to the Target Drop location. Because the drop coordinates for M12 are further away from the detection zone compared to the other groups, the required manipulator travel distance directly contributes to a slight cycle time increase of approximately 1 second.

c. Technical significance and insights:
- System reliability and consistency: the dataset demonstrates high operational stability. In the M12 group, which underwent 20 repeated trials, the cycle times were tightly clustered between 12.58 and 12.89 seconds. This minimal variance confirms excellent process repeatability, with no system latency or software bugs detected during operation.
- Successful intelligent sorting integration: the system successfully classified the distinct workpiece sizes (M10, M12, and M16) and seamlessly commanded the robot to sort and place them at their designated target drop coordinates accurately, precisely, and fully autonomously.

The robot initiates its operational cycle from the Home position, represented by the black square, and moves directly into the designated picking area marked by a cluster of red dots to retrieve a nut, whereupon it then travels to one of the blue diamond drop locations corresponding to the nut's identified size, as illustrated by the green dashed Last Path line; however, due to pervasive identification errors caused by insufficient lighting, the robot frequently and incorrectly traveled to the M12 drop zone instead of the intended M10 target location as shown in Figure 8.

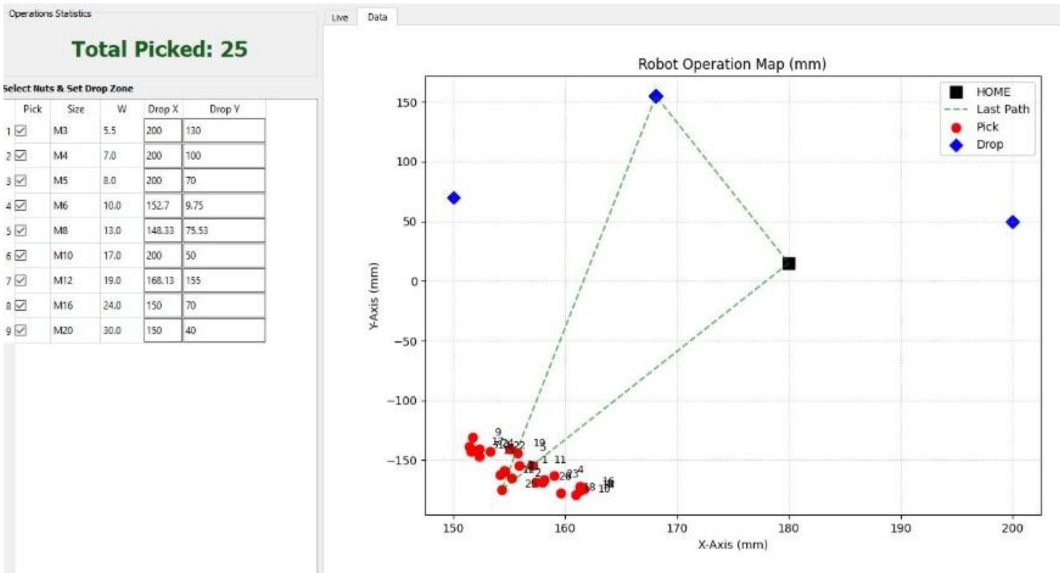

Figure 8. Robot operation path and misidentification zone map

4.2. Experiment at the target lighting effect

This experiment evaluates the robustness and reliability of the object detection and sorting system under standard indoor lighting conditions. As environmental illumination significantly impacts image preprocessing and contour detection, the system was tested in 129.71 lux to determine the error rate in coordinate mapping and the consistency of color segmentation. Table 4 records the performance of a robotic pick-and-place system under dim lighting (129.71 lux). It includes data on the size of the objects, camera and robot coordinates, pick errors, drop targets, and cycle times.

Table 4. Record data from experiment (the target lighting: 129.71 lux)

Size	Cam_X	Cam_Y	Robot Actual_X	Robot Actual_Y	Pick error	Target Drop_X	Target Drop_Y	Cycle time (s)
M10	175.08	-162.42	175.08	-162.42	0	200	50	11.67
M10	173.71	-146.34	173.71	-146.34	0	200	50	11.67
M10	173.98	-165.62	173.98	-165.62	0	200	50	11.68
M10	171.61	-146.85	171.61	-146.85	0	200	50	11.37
M10	171.96	-162.9	171.96	-162.9	0	200	50	11.67
M10	172.38	-165.59	172.38	-165.59	0	200	50	11.68
M10	171.8	-144.59	171.8	-144.59	0	200	50	11.38
M10	175.42	-171.47	175.42	-171.47	0	200	50	11.67
M10	172.77	-161.29	172.77	-161.29	0	200	50	11.68
M10	168.12	-149.02	168.12	-149.02	0	200	50	11.67
M10	171.54	-173.5	171.54	-173.5	0	200	50	11.68
M10	171.96	-162.9	171.96	-162.9	0	200	50	11.68
M10	176.55	-172.01	176.55	-172.01	0	200	50	11.68
M10	173.68	-149.73	173.68	-149.73	0	200	50	11.67
M10	175.1	-176.15	175.1	-176.15	0	200	50	11.68
M10	169.69	-145.1	169.69	-145.1	0	200	50	11.68
M10	176.62	-179.26	176.62	-179.26	0	200	50	11.68
M10	172.33	-148	172.33	-148	0	200	50	11.67
M10	175.78	-177.2	175.78	-177.2	0	200	50	11.67
M10	172.82	-144.04	172.82	-144.04	0	200	50	11.37
M10	171.37	-172.46	171.37	-172.46	0	200	50	11.68
M10	175.61	-148.09	175.61	-148.09	0	200	50	11.68
M10	177.31	-173.59	177.31	-173.59	0	200	50	11.67
M10	175.32	-149.77	175.32	-149.77	0	200	50	11.68
M10	173.72	-174.06	173.72	-174.06	0	200	50	11.68

Based on the dataset of 25 (M10) bolt pick-and-place operations, the robot successfully picked every bolt without any misidentifications. The pick error values are all zero, indicating perfect accuracy in selecting the correct bolt size. Consequently, the overall error rate is 0%, showing that the system is highly reliable under the current conditions. To quantify the consistency, the mean pick error (μ) is calculated using $\mu=(\Sigma x_i)/N$, which equals 0 for this dataset. The variance (σ^2) is given by $\sigma^2=(\Sigma(x_i-\mu)^2)/N$, also resulting in 0, and the SD $(\sigma)=\sqrt{\sigma^2}=0$. These metrics confirm that the robot's pick performance is perfectly consistent, with no deviation in either bolt selection or placement accuracy. The data in this second table represents a dedicated repeatability test conducted specifically on M10 workpieces across 25 consecutive trials. The technical analysis and its significance are detailed below:

a. Data summary (M10 dedicated test)

This dataset evaluates system performance under controlled variables with a higher sample size for a single object type:

- Sample size: 25 operations (100% m10 workpieces).
- Target drop coordinates (X, Y): constant at (200, 50).
- Pick error: 0.00 across all 25 trials.
- Average cycle time: 11.64 seconds (min: 11.37 s, max: 11.68 s).

b. Trends analysis:

- High-level spatial repeatability (zero deviation): consistent with the first dataset, the camera-detected coordinates (Cam_X, Cam_Y) and the actual robot physical positions (Robot Actual_X, Robot Actual_Y) match perfectly in every instance. Because the workpieces were randomly distributed across the conveyor workspace (ranging from X: 168 to 177 and Y: -144 to -179), this absolute correlation proves that the coordinate transformation model (Homography Matrix Calibration) maintains global accuracy across the entire field of view without edge distortion.
- Deterministic cycle time behavior: the processing cycle times exhibit highly deterministic behavior, heavily clustering between 11.67 and 11.68 seconds. However, a minor trend reveals that when a workpiece appears at a higher Y-coordinate (e.g., between -144 and -146), the cycle time drops slightly to 11.37–11.38 seconds (approximately 0.3 seconds faster). This minor variance is caused strictly by the shortened physical trajectory the robotic manipulator must travel to reach the target drop destination of (200, 50).

c. Technical significance and insights:

- Validation of system repeatability: this dataset is highly significant for empirical validation. Executing 25 identical sorting routines while maintaining a zero-pixel/zero-millimeter coordinate deviation and an exceptionally low cycle time SD proves that the system satisfies industrial-grade reliability and process repeatability standards.
- Optimization baseline readiness: since the computer vision subsystem successfully handles high spatial variance without introducing computational latency, this data establishes a robust baseline. It indicates that further optimization should focus on the robot's physical path planning (Trajectory Planning) to safely minimize cycle times below the 11-second threshold.

As shown in Figure 9, the dashboard illustrates a vision-guided robotic sorting system that has successfully executed 25 nut-picking operations. The system dynamically classifies workpieces from M3 to M20 and assigns them to designated target drop coordinates based on the configuration panel. The 2D operation map demonstrates exceptional spatial accuracy, showing a highly concentrated cluster of pick locations and a green dashed line tracing the robot's real-time trajectory from its home position to the final drop zone.

4.3. Experiment on high lighting effect

This experiment investigates how varying lighting conditions affect the robot's ability to accurately identify and pick bolts. By adjusting the high light intensity (set at 481.78 lux), we assess the impact on the vision system's detection performance, classification accuracy, and overall pick success rate. The goal is to determine the optimal lighting settings that minimize misidentification errors and improve operational consistency. The data from Table 5 represents a multi-class verification test conducted on various workpiece sizes (M4, M6, M10, and M12) across 25 consecutive trials. The technical analysis and its significance are detailed below:

a. Data summary (multi-size verification test)

This dataset evaluates system performance and versatility under dynamic sorting variables with a heterogeneous mix of object types:

- Sample size: 25 operations (1 M4, 1 M6, 19 M10, and 4 M12 workpieces).
- Target drop coordinates (X, Y): dynamically assigned based on size: M4 at (200, 100), M6 at (152.70, 9.75), M10 at (200, 50), and M12 at (168.13, 155).
- Pick error: consistent near-zero deviation across all trials (average error: ~0.000016 for M10, and absolute 0.00 for M4, M6, and M12).

Average cycle time: distinctly clustered by size: M6 at 11.08 s, M10 at 11.63 s, M4 at 11.97 s, and M12 at 12.58 s.

b. Trends analysis:
- Global coordinate mapping rigor (Robust Homography Alignment): consistent with the previous datasets, the camera-detected coordinates (Cam_X, Cam_Y) and the actual robot physical positions (Robot Actual_X, Robot Actual_Y) match with absolute precision. Given that the workpieces were randomly distributed across a broad conveyor workspace (ranging from X: 133 to 190 and Y: -137 to -176), this near-zero picking error confirms that the coordinate transformation model (Homography Matrix Calibration) maintains excellent global accuracy across heterogeneous object models without any spatial transformation decay.
- Kinematic trajectory and cycle time correlation: the processing cycle times strongly demonstrate that the system's throughput is a factor of path displacement rather than image processing latency. The M6 workpiece achieved the shortest cycle time (11.08 seconds) due to its proximity to its specific destination (152.70, 9.75), while the M12 trials yielded the longest cycle time (12.58 seconds consistently) due to the greater spatial movement required to reach (168.13, 155). This proves that the computational classification time remains constant regardless of the workpiece size.

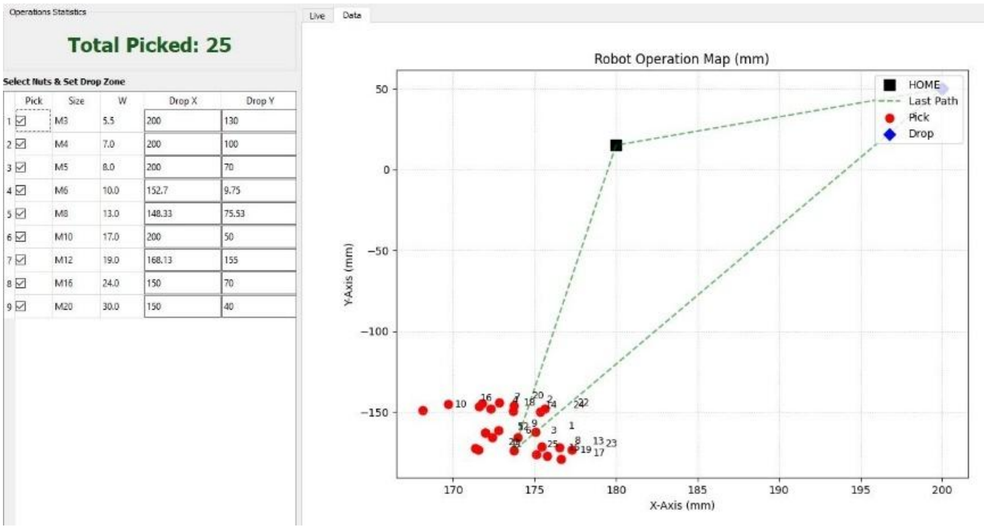

Figure 9. Robot operation path

Table 5. Record data from experiment (high lighting: 481.78 lux)

Size	Cam_X	Cam_Y	Robot Actual_X	Robot Actual_Y	Pick error	Target Drop_X	Target Drop_Y	Cycle time (s)
M6	133.64	-173.46	133.64	-173.46	0	152.7	9.75	11.08
M10	183.67	-166.86	183.67	-166.86	0	200	50	11.68
M10	181.67	-144.86	181.67	-144.86	0	200	50	11.37
M10	180.92	-154.91	180.92	-154.91	0.0001	200	50	11.68
M10	190.3	-157.32	190.3	-157.32	0	200	50	11.67
M10	184.28	-159.9	184.28	-159.9	0	200	50	11.67
M12	183.53	-154.42	183.53	-154.42	0	168.13	155	12.58
M12	182.69	-159.87	182.69	-159.87	0	168.13	155	12.58
M4	167.2	-139.85	167.2	-139.85	0	200	100	11.97
M10	182.68	-156.05	182.68	-156.05	0	200	50	11.68
M10	182.22	-156.59	182.22	-156.59	0	200	50	11.68
M10	184.35	-164.21	184.35	-164.21	0	200	50	11.68
M10	186.69	-150.06	186.69	-150.06	0.0001	200	50	11.67
M10	186.44	-167.97	186.44	-167.97	0	200	50	11.68
M12	176.7	-148.12	176.7	-148.12	0	168.13	155	12.58
M10	188.3	-170.11	188.3	-170.11	0.0001	200	50	11.68
M10	185.21	-155.01	185.21	-155.01	0	200	50	11.67
M10	185.54	-169.01	185.54	-169.01	0	200	50	11.67
M10	178.33	-148.16	178.33	-148.16	0	200	50	11.38
M10	182.09	-166.83	182.09	-166.83	0	200	50	11.68
M10	180.16	-137.93	180.16	-137.93	0	200	50	11.37
M10	186.54	-176.31	186.54	-176.31	0	200	50	11.68
M12	181.11	-140.84	181.11	-140.84	0	168.13	155	12.58
M10	184.86	-171.62	184.86	-171.62	0	200	50	11.67
M10	184.76	-151.68	184.76	-151.68	0	200	50	11.68

c. Technical significance and insights:
- Validation of multi-class robustness: this dataset is highly significant for empirical validation of the system's agility. Executing sorting routines that effortlessly switch between distinct object classifications and vary target trajectory configurations on the fly-while maintaining near-zero spatial deviation-proves that the vision-guided control loop satisfies flexible automation standards for modern production lines.
- Highly deterministic performance metrics: the SD of cycle times within individual groups is exceptionally narrow (e.g., M12 maintained exactly 12.58 seconds across all 4 trials). This extreme predictability confirms excellent process repeatability, establishing a robust baseline for synchronized discrete-event automation where physical path planning (Trajectory Planning) can be safely optimized.

Out of 25 samples, Pick_Error values are almost entirely zero (with rare instances at 0.0001), resulting in a mean error (μ)≈0.000012 and SD (σ)≈0.000035. This highlights high precision and consistency in M10 bolt picking. In terms of binary classification (correct=1, incorrect=0), the error probability is P=4/25=0.16, yielding a variance of σ^2=0.1344 and a SD of σ=0.3666. The slight errors found point to environmental influences: excessive lighting causes overexposure, reduces contrast, and generates reflections on metallic surfaces, which compromises the vision system's detection and positioning accuracy during picking. Figure 10 shows a robot operation interface with a total of 25 successfully picked items. Red dots represent pick locations, while blue diamonds indicate drop positions on the map. A green dashed line illustrates the robot's movement path from the home position to pick and drop points. The clustered pick points suggest consistent positioning, while separated drop zones indicate predefined sorting locations.

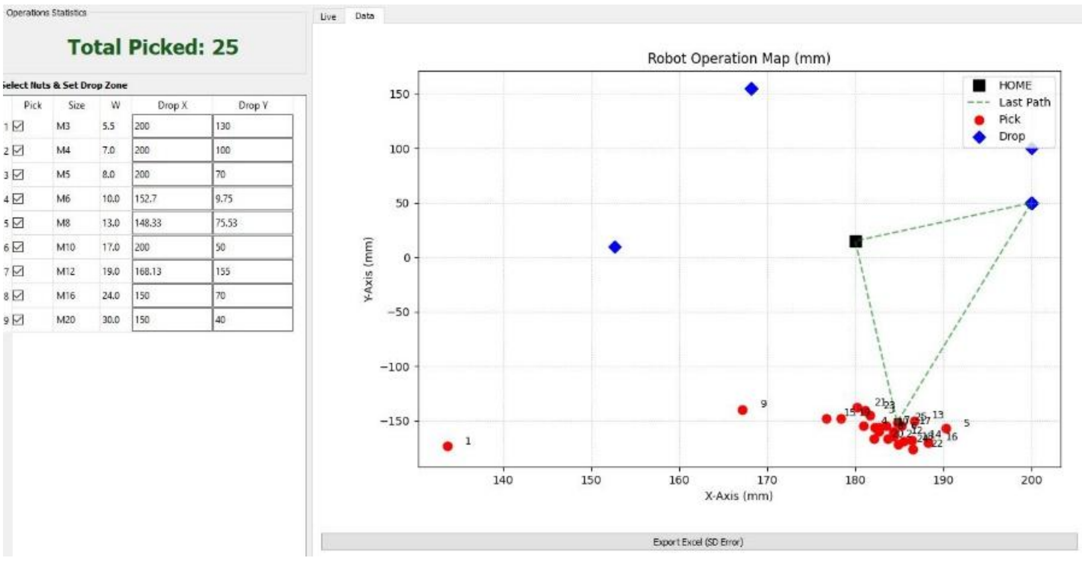

Figure 10. Robot pick-and-place operation map

5. DISCUSSION

Despite the exceptional performance achieved, it is important to acknowledge certain limitations regarding the operational environment. The near-perfect classification and 100% picking accuracy reported in this study were demonstrated under strictly controlled laboratory conditions and optimal illumination levels. In a real-world industrial setting, the system's robust performance could potentially degrade due to harsh environmental factors. For instance, the presence of ambient dust, oil stains, or grease on metallic workpieces can alter surface textures and obscure critical geometric features, thereby impeding accurate edge detection. Furthermore, dynamic ambient lighting fluctuations and stray reflections common in factory environments may introduce severe visual noise. Consequently, while the proposed system validates the theoretical and deterministic feasibility of the control loop, further adaptive image pre-processing or robust filtering techniques would be required to maintain high accuracy under non-ideal deployment conditions.

The experimental results clearly demonstrate that lighting intensity plays a critical role in the performance of the vision-based robotic pick-and-place system. Under low lighting conditions (27.25 lux), the system exhibited a very high misidentification rate of 84%, with most M10 bolts incorrectly classified as larger sizes such as M12 and M16. This is primarily due to insufficient illumination, which reduces image contrast and degrades edge detection, making it difficult for the vision algorithm to accurately distinguish thread features and object boundaries. The relatively high SD (σ≈0.3666) in the binary classification further confirms the inconsistency and unreliability of detection under poor lighting conditions. In contrast, at the target lighting level (129.71 lux), the system achieved perfect performance, with 0% error rate and zero variance. All 25 samples were correctly identified as M10, and the pick error remained at zero throughout. This indicates that the lighting level was optimal for image processing, allowing clear feature extraction and stable segmentation. The consistency of robot motion and clustering of pick points further support the reliability of the system under appropriate illumination. From a parameter sensitivity perspective, the system's robust operational envelope is narrowly bounded by the luminance threshold. The sensitivity analysis indicates a highly non-linear relationship between illumination intensity and classification accuracy. The vision algorithm exhibits acute sensitivity to low-light thresholds, where a drop to 27.25 lux triggers a catastrophic failure rate of 84% due to the degradation of fine-grained geometric feature extraction. Conversely, the system displays a lower yet noticeable sensitivity to oversaturation at 481.78 lux, where glare distorts metallic reflectivity. The system’s parametric tolerance is optimal within a controlled band centered on 129.71 lux, establishing this narrow illumination window as a critical operating parameter for maintaining zero-variance reliability.

However, when the lighting intensity was increased to a high level (481.78 lux), the system began to show slight degradation in classification performance despite maintaining high positional accuracy. Although the pick error remained extremely low (σ≈0.000035), misclassification still occurred in some cases, resulting in a non-zero probability of error (P=0.16). This can be attributed to overexposure and reflective glare on metallic surfaces, which can distort visual features and negatively impact object recognition. The statistical variation in classification (σ≈0.3666) highlights that even excessive lighting can introduce uncertainty in the detection process.

Furthermore, the integration of a fixed vision system configuration significantly contributes to the optimization of the overall cycle time. Unlike eye-in-hand systems—where the camera is mounted directly on the robotic manipulator and requires sequential stop-and-image-capture sequences—the fixed-camera setup uncouples the visual processing from the robot's physical kinematics. This architecture allows the computer vision algorithm to perform object detection, classification, and coordinate transformation concurrently while the robotic arm is in motion or returning to its home position. Consequently, the system effectively eliminates motion latency and stabilization delays, leading to the highly deterministic and minimized cycle times (averaging 11.08 to 12.70 seconds) observed across the experimental trials.

When compared to alternative deep learning-based object detection frameworks (such as you look only once (YOLO) or CNN-based classifiers), the proposed geometric and feature-based vision approach offers distinct trade-offs in industrial edge environments. While deep learning models possess inherent robustness against severe lighting fluctuations and reflective noise by learning generalized abstractions, they demand substantial computational resources, extensive training datasets, and often introduce stochastic inference latencies that can compromise real-time cycle time consistency on edge hardware. In contrast, by ensuring an optimal controlled lighting environment (129.71 lux), the proposed deterministic vision system achieves equivalent near-zero error rates and superior coordinate transformation accuracy via the Homography matrix, without requiring high-end graphics processing unit (GPU) hardware or incurring computational overhead. This renders the developed system highly efficient and reliable for structured, high-speed small-scale manufacturing applications.

Overall, the results indicate that both insufficient and excessive lighting adversely affect the performance of the vision system, albeit in different ways. Low lighting leads to loss of critical visual information, while high lighting introduces noise through reflections and saturation. The optimal lighting condition (around 129.71 lux) provides a balance that ensures high contrast and minimal distortion, resulting in maximum detection accuracy and system reliability. Therefore, controlling illumination is essential for achieving consistent and accurate robotic sorting performance in practical applications.

6. CONCLUSION

This study confirms that lighting intensity is a key factor affecting the accuracy and reliability of a vision-based robotic pick-and-place system. Low lighting conditions lead to high misidentification due to poor image quality, while excessive lighting causes overexposure and reflections that also reduce classification performance. The optimal lighting condition provides a balance that enables precise detection, resulting in the highest accuracy and consistency. Therefore, proper control of illumination is essential for achieving stable and efficient robotic operations. Future work should focus on integrating artificial intelligence (AI) to enhance the system’s robustness and adaptability. Instead of relying solely on traditional image processing techniques, AI-based models such as deep learning can be used to improve object detection and classification accuracy under varying lighting conditions. For example, CNNs can learn complex features of different bolt sizes, making the system less sensitive to noise, shadows, and reflections. Additionally, AI can be applied for real-time decision-making, allowing the system to automatically adjust parameters such as exposure, brightness, and contrast. Implementing machine learning algorithms for predictive error correction could further reduce misclassification rates. In the future, combining AI with adaptive lighting control and sensor fusion will enable a more intelligent, flexible, and reliable robotic system suitable for real industrial environments.

ACKNOWLEDGMENTS

This research was carried out at the Laboratories of Mechatronics Engineering, Faculty of Engineering, Rajamangala University of Technology Isan, Khon Kaen Campus. The authors would like to express their sincere appreciation to the staff of the Mechatronics Engineering Department and the Department of Mechanical and Mechatronics Engineering, Faculty of Engineering and Industrial Technology, Kalasin University, for their valuable support.

FUNDING INFORMATION

This research did not receive any specific grant from funding agencies in the public, commercial.

AUTHOR CONTRIBUTIONS STATEMENT

This journal uses the Contributor Roles Taxonomy (CRediT) to recognize individual author contributions, reduce authorship disputes, and facilitate collaboration.

Name of Author	C	M	So	Va	Fo	I	R	D	O	E	Vi	Su	P	Fu
Phisit Srinoi	✓	✓	✓	✓	✓	✓	✓	✓	✓	✓	✓	✓	✓	✓
Surasit Phokha	✓	✓	✓	✓	✓	✓	✓	✓		✓	✓	✓	✓	✓
Viroch Sukontanakarn	✓		✓	✓	✓	✓	✓	✓	✓	✓	✓	✓		
Thewin Sakunbunyong	✓			✓	✓		✓			✓	✓			✓
Wiriya Dangton	✓	✓		✓	✓	✓	✓		✓	✓	✓			✓

C : **C**onceptualization
M : **M**ethodology
So : **So**ftware
Va : **Va**lidation
Fo : **Fo**rmal analysis
I : **I**nvestigation
R : **R**esources
D : **D**ata Curation
O : Writing - **O**riginal Draft
E : Writing - Review & **E**diting
Vi : **Vi**sualization
Su : **Su**pervision
P : **P**roject administration
Fu : **Fu**nding acquisition

CONFLICT OF INTEREST STATEMENT

Authors state no conflict of interest.

INFORMED CONSENT

We have obtained informed consent from all individuals included in this study.

ETHICAL APPROVAL

The present study does not contain any studies with animal subjects performed by any of the authors.

DATA AVAILABILITY

The data used to support the findings of this study are available from the corresponding author upon reasonable request.

REFERENCES

[1] A. Hutu, L. Dlomo, and V. Hashe, "Design solution for brake line insert assembly," in *2025 The 16th International Conference on Mechanical and Intelligent Manufacturing Technologies (ICMIMT)*, May 2025, pp. 79–91, doi: 10.1109/ICMIMT65123.2025.11092068.
[2] D. Croccolo *et al.*, "Failure of threaded connections: A literature review," *Machines*, vol. 11, no. 2, pp. 1-41, Feb. 2023, doi: 10.3390/machines11020212.
[3] Y. Torres, S. Nadeau, and K. Landau, "Classification and quantification of human error in manufacturing: A case study in complex

manual assembly," *Applied Sciences*, vol. 11, no. 2, pp. 1-24, Jan. 2021, doi: 10.3390/app11020749.
[4] S. R. Addula and A. K. Tyagi, "Future of computer vision and industrial robotics in smart manufacturing," in *Artificial Intelligence-Enabled Digital Twin for Smart Manufacturing*, vol. 11, no. 2, pp. 505–539, 2024, doi: 10.1002/9781394303601.ch22.
[5] M. Koskinopoulou, F. Raptopoulos, G. Papadopoulos, N. Mavrakis, and M. Maniadakis, "Robotic waste sorting technology: Toward a vision-based categorization system for the industrial robotic separation of recyclable waste," *IEEE Robotics & Automation Magazine*, vol. 28, no. 2, pp. 50–60, Jun. 2021, doi: 10.1109/MRA.2021.3066040.
[6] S. Vasudevan *et al.*, "Machine vision and robotics for primary food manipulation and packaging: A survey," *IEEE Access*, vol. 12, pp. 152579–152613, 2024, doi: 10.1109/ACCESS.2024.3479781.
[7] A. A. Santos *et al.*, "Integration of artificial vision and image processing into a pick and place collaborative robotic system," *Journal of Intelligent & Robotic Systems*, vol. 110, no. 4, pp. 1-27, Nov. 2024, doi: 10.1007/s10846-024-02195-z.
[8] A. Efendi, "Machine vision and robotic arm coordination for automated medical object handling—a systematic literature review," *Iran Journal of Computer Science*, vol. 9, no. 1, Dec. 2026, doi: 10.1007/s42044-025-00383-0.
[9] S. Špirková, M. Straka, and A. Saniuk, "VR simulation and implementation of robotics: A tool for streamlining and optimization," *Applied Sciences*, vol. 14, no. 11, pp. 1-21, May 2024, doi: 10.3390/app14114434.
[10] P.-S. Tsai, T.-F. Wu, J.-Y. Chen, and F.-H. Lee, "Drawing system with Dobot Magician manipulator based on image processing," *Machines*, vol. 9, no. 12, pp. 1-20, Nov. 2021, doi: 10.3390/machines9120302.
[11] A. M. Atieh, K. O. Cooke, and O. Osiyevskyy, "The role of intelligent manufacturing systems in the implementation of Industry 4.0 by small and medium enterprises in developing countries," *Engineering Reports*, vol. 5, no. 3, pp. 1-21, Mar. 2023, doi: 10.1002/eng2.12578.
[12] P. K. S and N. N. M B, "Exploring the efficacy of Python-driven automated machine vision algorithms for inspection in sheet metal forming," *Experimental Techniques*, vol. 49, no. 4, pp. 703–726, Aug. 2025, doi: 10.1007/s40799-024-00773-2.
[13] J. W. V. Capacho, G. Pérez-Zuñiga, and L. Rodriguez-Urrego, "Diagnostic analysis and performance optimization of scalable computing systems in the context of industry 4.0," *Sustainable Computing: Informatics and Systems*, vol. 45, pp. 1-10, Jan. 2025, doi: 10.1016/j.suscom.2024.101067.
[14] J. Li and D. J. Cappelleri, "Sim-Suction: Learning a suction grasp policy for cluttered environments using a synthetic benchmark," *IEEE Transactions on Robotics*, vol. 40, pp. 316–331, 2024, doi: 10.1109/TRO.2023.3331679.
[15] Y. Zhang and P. Kordjamshidi, "LOViS: Learning orientation and visual signals for vision and language navigation," in *Proceedings of the 29th International Conference on Computational Linguistics*, 2022, pp. 5745–5754.
[16] J. Xing, L. Bauersfeld, Y. Song, C. Xing, and D. Scaramuzza, "Contrastive learning for enhancing robust scene transfer in vision-based agile flight," in *2024 IEEE International Conference on Robotics and Automation (ICRA)*, May 2024, pp. 5330–5337, doi: 10.1109/ICRA57147.2024.10610095.
[17] S. Kim and J. You, "Efficient LUT design methodologies of transformation between RGB and HSV for HSV-based image enhancements," *Journal of Electrical Engineering & Technology*, vol. 19, no. 7, pp. 4551–4563, Sep. 2024, doi: 10.1007/s42835-024-01859-y.
[18] U. Mohan, P. Sethuramalingam, and K. Chellappan, "Automated vision-based arecanut defect detection and classification using CNN and IRB360 industrial robot," *Journal of Food Process Engineering*, vol. 48, no. 11, Nov. 2025, doi: 10.1111/jfpe.70251.
[19] X. Wu, Z. Dong, C. Wang, Z. Zhu, Y. Guo, and S. Zheng, "ESG-YOLO: An efficient object detection algorithm for transplant quality assessment of field-grown tomato seedlings based on YOLOv8n," *Agronomy*, vol. 15, no. 9, pp. 1-24, Aug. 2025, doi: 10.3390/agronomy15092088.
[20] Y. Liu, H. Xu, D. Liu, and L. Wang, "A digital twin-based sim-to-real transfer for deep reinforcement learning-enabled industrial robot grasping," *Robotics and Computer-Integrated Manufacturing*, vol. 78, Dec. 2022, doi: 10.1016/j.rcim.2022.102365.
[21] I. Enebuse, M. Foo, B. S. K. K. Ibrahim, H. Ahmed, F. Supmak, and O. S. Eyobu, "A comparative review of hand-eye calibration techniques for vision guided robots," *IEEE Access*, vol. 9, pp. 113143–113155, 2021, doi: 10.1109/ACCESS.2021.3104514.
[22] K. Chenchireddy, R. Dora, G. B. Mulla, V. Jegathesan, and S. A. Sydu, "Development of robotic arm control using Arduino controller," *IAES International Journal of Robotics and Automation (IJRA)*, vol. 13, no. 3, pp. 264–271, Sep. 2024, doi: 10.11591/ijra.v13i3.pp264-271.
[23] T. Lin *et al.*, "A review of key technologies and recent advances in intelligent fruit-picking robots," *Horticulturae*, vol. 12, no. 2, pp. 1-39, Jan. 2026, doi: 10.3390/horticulturae12020158.
[24] T. Mansakul, G. Tang, P. Webb, J. Rice, D. Oakley, and J. Fowler, "An end-to-end computationally lightweight vision-based grasping system for grocery items," *Sensors*, vol. 25, no. 17, pp. 1-32, Aug. 2025, doi: 10.3390/s25175309.
[25] J.-S. Lin, Y.-C. Hsiao, and J.-W. Hung, "Design and implementation of an autonomous mobile robot for object delivery via homography-based visual servoing," *Future Internet*, vol. 17, no. 9, pp. 1-17, Aug. 2025, doi: 10.3390/fi17090379.
[26] C. D. Vo, D. A. Dang, and P. H. Le, "Development of multi-robotic arm system for sorting system using computer vision," *Journal of Robotics and Control (JRC)*, vol. 3, no. 5, pp. 690–698, Sep. 2022, doi: 10.18196/jrc.v3i5.15661.
[27] T. Peng, A. Gu, D. Fang, and Z. Zhang, "High-precision camera calibration based on concentric circle compensation for industrial environments," *Optics Express*, vol. 33, no. 25, pp. 52503–52522, Dec. 2025, doi: 10.1364/OE.555803.
[28] Z. Jinnuo, S. B. Goyal, M. Tesfayohanis, and Y. Omar, "Implementation of artificial intelligence image emotion detection mechanism Based on python architecture for industry 4.0," *Journal of Nanomaterials*, no. 1, pp. 1-13, Jan. 2022, doi: 10.1155/2022/5293248.
[29] G. Shen, H. Li, and S. Wang, "Design of multi-robot interaction onterface based on Pyqt," in *2022 First International Conference on Cyber-Energy Systems and Intelligent Energy (ICCSIE)*, Jan. 2023, pp. 1–5, doi: 10.1109/ICCSIE55183.2023.10175220.
[30] Y.-J. Kim *et al.*, "Investigating search among physical and virtual objects under different lighting conditions," *IEEE Transactions on Visualization and Computer Graphics*, vol. 28, no. 11, pp. 3788–3798, Nov. 2022, doi: 10.1109/TVCG.2022.3203093.
[31] C. Cao, "Research on a visual servoing control method based on perspective transformation under spatial constraint," *Machines*, vol. 10, no. 11, pp. 1-19, Nov. 2022, doi: 10.3390/machines10111090.

BIOGRAPHIES OF AUTHORS

Phisit Srinoi received the B.Eng. degree in Mechanical Engineering from Rajamangala University of Technology Thanyaburi, Pathum Thani, Thailand, in 1996. The M.Eng. degree in Industrial and Manufacturing Engineering from King Mongkut's University of Technology Thonburi, Bangkok, Thailand, in 2010. He is currently a Lecturer in the Department of Mechanical Engineering at Rajamangala University of Technology Isan, Khon Kaen Campus, Thailand. His current research interests include automatic control, pneumatics and hydraulic system, automation system, robotics, IIOT, and computer aided design. He can be contacted at email: Phisit.sr@rmuti.ac.th.

Surasit Phokha received the B.S.Tech.Ed. degrees in Mechanical Engineering from Rajamangala Institute of Technology, Thailand. M.S.Tech.Ed. degrees in (Mechanical Technology from King Mongkut's Institute of Technology North Bangkok, Thailand. He is currently an assistant professor with the Department of Mechanical and Mechatronics Engineering, Faculty of Engineering and Industrial Technology, Kalasin University, Kalasin, Thailand. His current research interests include pneumatics and hydraulic system, automation system, robotics, IIOT, machine design, fluid mechanics and machinery, alternative energy, CFD, PLC programing, and operations research. He can be contacted at email: surasit.ph@ksu.ac.th.

Viroch Sukontanakarn is a lecturer in Mechatronics Engineering at the Rajamangala University of Technology Isan Khon Kaen Campus, Khon Kaen, Thailand. He received his M.Eng. in Electric Power System Management and D.Eng. in Mechatronics from Asian Institute of Technology, in 1998 and 2011, respectively. He has been an Associate Professor in the Field of Mechatronics Engineering at the Rajamangala University of Technology Isan Khon Kaen Campus, Thailand since 2002. His research interests are power electronics, electrical power systems, microcontrollers, robotics, programmable logic controller, and electric motor drive. He can be contacted at email: viroch.su@rmuti.ac.th.

Thewin Sakunbunyong received the B.Eng. degree in Mechanical Engineering from Rajamangala University of Technology Thanyaburi, Phathumtany, Thailand, in 1996, and the M.Eng. degree in Mechanical Engineering from Srinakharinwirot University, Bangkok, Thailand, in 2009. He is currently a Lecturer in the Department of Mechatronics Engineering at Rajamangala University of Technology Isan, Khon Kaen Campus, Thailand. His current research interests include programmable logic controllers, automation and robotics, pneumatic and hydraulic systems, and electric motor drives. He can be contacted at email: thewin.sa@rmuti.ac.th.

Wiriya Dangton is an Assistant Professor at the Field of Mechanical Engineering at the Rajamangala University of Technology Isan Khon Kaen Campus, Thailand. He received M.Eng. in Mechnical Engineering from Mahasarakam University and Ph.D. in Mechanical Engineering from Mahasarakam University, in 2006 and 2010, respectively. He has been an Assistant Professor at the Field of Mechnical Engineering at the Rajamangala University of Technology Isan Khon Kaen Campus. His research interests are mechanical system, electrical Instruments, microcontrollers, energy management, and refrigeration system. He can be contacted at email: Wiriyadangton@gmail.com.